ЖЭТФ, 2021, том 160, вып. 3 (9), стр. 366–371 

# GAMMA-RAYS AND NEUTRINOS FROM PROTON–PROTON INTERACTIONS IN GAMMA-RAY BURSTS

***A. Neronov*** [a,b*], ***Y. Gatelet*** [a]

[a] *APC, University of Paris, CNRS/IN2P3, CEA/IRFU 75205, Paris, France*

[b] *Astronomy Department, University of Geneva CH-1290, Versoix, Switzerland*

Received November 9, 2020,
revised version December 18, 2020.
Accepted for publication December 21, 2020

**DOI:** 10.31857/S0044451021090030

Expansion of relativistic outflows of gamma-ray bursts (GRB) into medium created by the winds or their progenitor stars is accompanied by interactions of picked-up protons with the medium. These interactions produce neutrinos and $\gamma$-rays with energies in the TeV–PeV range. We study if such neutrinos and $\gamma$-rays are detectable with neutrino and $\gamma$-ray telescopes. We find that neutrino signal can be detectable with IceCube-Gen2 type telescope(s) if the GRB progenitor has been a low-metallicity star with initial mass $(40–100)M_\odot$, or if the progenitor system has been a binary with dense circumstellar environment ($\sim 10^{13}$ cm$^{-3}$) within the binary system extent. $\gamma$-ray emission from pion decays is detectable only in the afterglow phase, because of the pair production opacity of the prompt emission. This emission can contribute to the TeV afterglow flux of GRBs. Detection of the pion decay $\gamma$-ray and neutrino emission can serve as a diagnostic of the GRB progenitor evolution during the last years of its life.

Before the gravitational collapse, massive stars experience significant wind-like and explosive mass loss [1]. These stars are perhaps progenitors of long gamma-ray bursts (GRB) [2–4]. GRB relativistic outflow might propagate through matter-rich circumstellar environment created by the stellar wind and interact with this environment [5].

Recent detection of very-high-energy (VHE) $\gamma$-ray emission from GRB 180720B [6, 7] and GRB 190114C [8,9] afterglows might potentially carry such signatures. The VHE $\gamma$-ray flux can hardly be attributed to the synchrotron emission that presumably forms the bulk of the GRB prompt and afterglow flux [3, 4, 10, 11], because the synchrotron spectrum can hardly extend into the VHE band. Alternatively, the inverse Compton emission [9, 12, 13] produced by electrons with extremely high Lorentz factors possibly accelerated at the forward shock of the GRB outflow is also not directly sensitive to the matter content of the medium through which the GRB outflow propagates.

It is also possible that in exceptional VHE-$\gamma$-ray-bright GRBs part of the $\gamma$-ray emission is produced by high energy proton interactions. Such emission is also not directly sensitive to the circumstellar environment if proton interact with radiation field through photo-pion production, as suggested in a range of hadronic models of GRBs [14]. To the contrary, proton–proton interactions are directly sensitive to the density of the circumstellar medium.

Proton–proton interactions are conventionally not considered in the GRB afterglow physics because of the assumption of collisionless propagation of the GRB outflow through external medium. However, Refs. [15–18] show that even if particle collisions do not affect the dynamics of the GRB outflow and particle acceleration processes, proton interactions still generate secondary particles taking small fraction of the blast wave energy. If the progenitor stellar system of the GRB has produced strong wind or evolved as a binary system just before the explosion, signatures of the *pp* interactions could be present in the GRB prompt-emission and/or afterglow spectral and timing properties. In what fol-

* E-mail: andrii.neronov@gmail.com

lows we explore these signatures. We show that $\gamma$-ray and neutrino emission from $pp$ interactions can reach detectable levels and provide a diagnostic of the presence of dense wind environment around the collapsed star generated by the mass loss prior to the collapse or by interactions with a companion star in a binary system.

The density of the circumstellar medium at the distance $r$ is determined by the mass loss rate at the time

$$t_w = \frac{r}{v_w} \simeq 10 \left[\frac{v_w}{300 \text{ km/s}}\right]^{-1} \left[\frac{r}{10^{16} \text{ cm}}\right] \text{ yr} \quad (1)$$

before the collapse, where $v_w$ is the wind velocity, cf. Refs. [19–23]. Emission from GRB outflow propagating at the distances $\sim 10^{16}$ cm from the collapsed star can potentially probe the history of mass ejection over the last decade of the progenitor star life.

GRB outflow expanding into the circumstellar medium initially goes through the "coasting" stage. During this stage, even if the GRB outflow is not initially loaded with protons, it starts to pick up and accelerate protons from the wind. The amount of material picked up after expansion to the distance $r$ is

$$N(r) = \Omega \int_{R_*}^{r} n(r')r'^2 dr' = \frac{n_0 \Omega R_*^\gamma r^{3-\gamma}}{3-\gamma}, \quad (2)$$

where $n_0$ is the central wind density, $R_* \sim 10^{12}$ cm and $\gamma \approx 2$ are the characteristic scale and the power-law exponent of the density profile. In the reference frame of the outflow, protons from the medium arrive all from radial direction with energy $E' = \Gamma_0 m_p$ where $\Gamma_0$ is the initial bulk Lorentz factor of the outflow. The picked up particles initially form a nearly monoenergetic isotropic distribution sharply peaked at the energy $E'$. Shock acceleration process may produce protons with still higher energies, so that the spectrum of protons may extend as a powerlaw above the energy $E'$. A conventional assumption is that the acceleration process results in a powerlaw spectrum $f'(E') \propto (E')^{-p}$, $p \simeq 2$ for $E' > \Gamma_0 m_p$. Uncertainties in the physics of relativistic shock acceleration yield large scatter of possible spectral slopes deviating from $p = 2$ [24].

If most of the kinetic energy of the picked up material is contained in particles with energies $E' \sim \Gamma_0 m_p$ in the comoving frame, the energy distribution of protons in the collapsar frame is peaked at the energy $E \sim \Gamma_0^2 m_p$. The total kinetic energy of the outflow grows as [25] $\mathcal{E}(r) \sim \Gamma_0^2 m_p N$. The total energy of the picked up protons gradually gets comparable to the total energy release of the GRB, $\mathcal{E}_0$. The upper limit on this energy is set by the overall energy liberated in the gravitational collapse, estimated as the gravitational binding energy of material forming the black hole confined to its horizon $R_{bh} \sim G_N M_{bh}/c^2$:

$$E_{grav} \sim G_N M_{bh}^2 / R_{bh} = M_{bh} c^2 \sim 10 M_\odot c^2 \sim 2 \cdot 10^{55} \text{ erg}.$$

As soon as the kinetic energy of the picked up material becomes comparable to the energy of the outflow, it starts to decelerate.

The "coasting" phase of the GRB outflow continues up to the distance $r_0$ at which $\mathcal{E}(r_0) \sim \mathcal{E}_0$:

$$r_0 = \left(\frac{(3-\gamma)\mathcal{E}_0}{\Gamma_0^2 m_p n_0 \Omega R_*^\gamma}\right)^{1/(3-\gamma)}. \quad (3)$$

The signal from within this distance is expected to arrive within the time interval

$$t_0 \sim \frac{r_0}{2\Gamma_0^2} \quad (4)$$

from the GRB start, possibly by the end of the prompt emission phase of the GRB. During the subsequent deceleration stage the outflow dynamics follows the Blandford–McKee solution [25] for an adiabatic relativistic blast wave. The bulk Lorentz factor of the blast wave decreases with distance $r$ and new particles picked up by the outflow gain energy $\Gamma(r)^2 m_p$. The particles which were initially picked up still might retain their energy $\sim \Gamma_0 m_p$ in the comoving frame, but in the collapsar frame their energy decreases down to maximum $E_r \sim \Gamma\Gamma_0 m_p$ (as could be found from the Lorentz transformation between the collapsar and comoving frames).

As a result, there is a specific spectrum of protons which establishes in the comoving frame in the absence of additional shock acceleration. Most of the energy distributed among the freshly picked up particles so that $\mathcal{E}_0 \simeq \Gamma^2 m_p N = \Gamma^2 m_p n_0 R_*^2 r$ for $\Gamma \ll \Gamma_0$. The distance dependence of the gamma-factor can be converted into time dependence for the observer's time $t$ using a relation $r(t)$ found from $dr = 2\Gamma^2 dt$ which gives $r = 2\Gamma^2 \left((4-\gamma)t - t_0\right)$ so that

$$\Gamma = \left(\frac{(3-\gamma)\mathcal{E}_0}{2^{3-\gamma} m_p n_0 R_*^\gamma \Omega \left[(4-\gamma)t - t_0\right]^{3-\gamma}}\right)^{1/(2(4-\gamma))} \quad (5)$$

scales at $t^{-1/4}$ in the case $\gamma = 2$.

The picked up protons carry the energy of the GRB outflow. They dissipate a part of this energy in $pp$ interactions. The energy output from these interactions is

$$\frac{d\mathcal{E}_{pp}}{dr} = \kappa\sigma_{pp} n \begin{cases} \Gamma_0^2 m_p N, & r < r_0, \\ \mathcal{E}_0, & r > r_0, \end{cases} \quad (6)$$

where $\sigma_{pp} \simeq 5 \cdot 10^{-26}$ cm$^2$ is the cross-section of $pp$ interactions and $\kappa \simeq 0.5$ is the average inelasticity of $pp$ collisions [26, 27].

We obtain the luminosity of

$$\mathcal{L}_{pp} = 2\kappa\Gamma^2\sigma_{pp} n\mathcal{E}_0 = = 2 \cdot 10^{48} \left[\frac{\Omega}{0.1}\right]^{1/2} \left[\frac{t}{7 \text{ s}}\right]^{-3/2} \left[\frac{\mathcal{E}_0}{10^{54} \text{ erg/s}}\right]^{1/2} \times \times \left[\frac{n_0}{10^{13} \text{ cm}^{-3}}\right]^{3/2} \left[\frac{R_*}{10^{12} \text{ cm}}\right]^3 \frac{\text{erg}}{\text{s}}. \quad (7)$$

The flux decreases as $t^{3/(4-\gamma)}$ at late times. If $\gamma = 2$ (environment created by the wind with constant mass loss rate) then the flux decrease is $t^{-3/2}$.

If the radial density profile of the medium has a shallower slope, e.g. $\gamma = 1$, the overall time dependence of $\mathcal{L}_{pp}$ changes. The luminosity grows as $t^{3-2\gamma} = t$ during the coasting phase and decreases as $t^{-3/(4-\gamma)} = t^{-1}$ during the deceleration phase (see (7)). The shallower profile of the stellar wind density can be e. g. due to the decrease of the mass loss rate of the progenitor star over the last 10 years before the gravitational collapse.

The luminosity $\mathcal{L}_{pp}$ deposited by the proton–proton interactions into neutrinos and electromagnetic channel is detectable by neutrino and gamma-ray telescopes. Most of the neutrino and $\gamma$-ray flux is initially concentrated in a decade-wide energy range at the energy $\lesssim 10\,\%$ of the proton energy [28], i. e. at

$$E_{\gamma,\nu} \lesssim 0.1\Gamma_0^2 m_p \simeq 4 \left[\frac{\Gamma_0}{200}\right]^2 \text{ TeV} \quad (8)$$

if there is no significant acceleration of protons.

Otherwise, if the shock acceleration process is efficient, the spectrum extends to higher energies as a powerlaw with the slope nearly identical to that of the accelerated proton spectrum.

The number of neutrino events per GRB in a detector of volume $V$ is

$$N_\nu \simeq 10^{-2} \left[\frac{A}{10^{37} \text{ cm}^{-1}}\right]^2 \left[\frac{D}{1 \text{ Gpc}}\right]^{-2} \left[\frac{V_{det}}{1 \text{ km}^3}\right]$$

for a GRB at the distance $D$, where $A = n_0 R_*^2$. This estimate shows that only exceptional GRBs occurring in dense extended circumstellar environment might yield $N_\nu \sim 1$ neutrino event statistics in neutrino detectors like IceCube, Baikal-GVD, or Km3NET. This might be the case e. g. for GRBs occurring in binary stellar systems, with density $n_0 \sim 10^{13}$ cm$^{-3}$ across large region of the size about the binary separation distance, $R_* \sim 3 \cdot 10^{12}$ cm can yield $N_\nu \sim 1$ neutrino signal. Otherwise, the dense circumstellar environment can also be found around low-metallicity progenitor stars in the mass range $40M_\odot - 100M_\odot$ for which the central wind densities can exceed $3 \cdot 10^{14}$ cm$^{-3}$ [21].

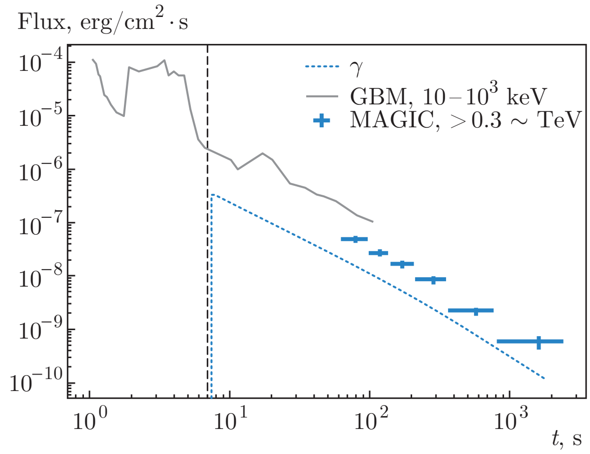


**Fig. 1.** (Color online) Fermi/GBM (grey solid line) and MAGIC (blue data points) lightcurves of GRB 190114C. Vertical dashed line marks the suggested time scale $t_0$ given by Eq. (4). Dotted blue line shows possible 0.3–1 TeV $\gamma$-ray flux for the reference $\pi^0$ decay model of GRB outflow propagating through the wind environment

Pion decay $\gamma$-rays which are initially produced in the same energy band as neutrinos do not escape from the source because of the pair production opacity of the GRB outflow, cf. Ref. [29–31]. TeV photons from $pp$ interactions produced in the prompt emission zone are immediately converted into $e^+e^-$ pairs which contribute to the pair loading of the GRB outflow and ultimately contribute to the prompt flux in the energy range in which the pair production optical depth is $\tau_{\gamma\gamma} \lesssim 1$.

$\gamma$-rays produced in $pp$ interactions during the deceleration phase of the GRB outflow lag behind the region occupied by the pulse of the prompt emission. Thus, they never interact with the prompt emission photons. During the deceleration phase the luminosity $L_\epsilon$ drops by several orders of magnitude, as illustrated by GRB 190114C (Fig. 1). This makes the GRB outflow transparent to the VHE $\gamma$-rays. If the luminosity $L_\epsilon$ decreases as $L_\epsilon = L_{\epsilon,0}(t/t_0)^{-\delta}$ during the afterglow phase, the optical depth scales as

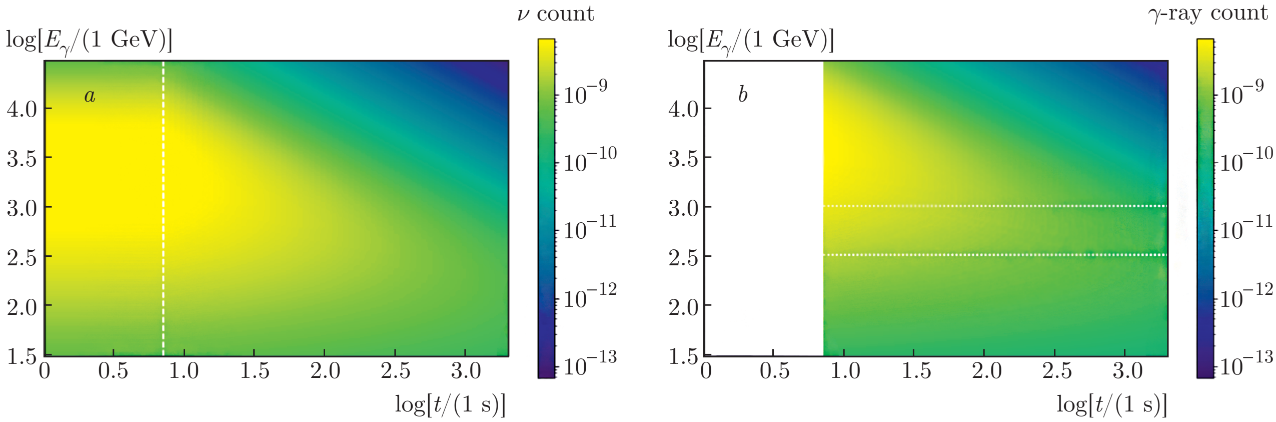


**Fig. 2.** (Color online) Spectral evolution of neutrino ($a$) and $\gamma$-ray ($b$) emission from $pp$ interactions. $Y$ axes show the neutrino or photon energy, $X$ axis is time. Color shows the spectral energy density. White vertical line marks the end of the coasting phase. White piece-wise straight lines show the evolution of the peak energy. White horizontal lines mark the energy range of MAGIC detection of GRB 190114C

$$\tau_{\gamma\gamma} \simeq 1 \left[\frac{L_{\epsilon,0}}{10^{51}\ \text{erg/s}}\right] \left[\frac{E_\gamma}{300\ \text{GeV}}\right] \times \\ \times \left[\frac{\Gamma}{200}\right]^{-6} \left[\frac{t}{10\ \text{s}}\right]^{-(1+\delta)} \quad (9)$$

and the outflow is transparent to the TeV $\gamma$-rays.

The requirement that opacity for TeV $\gamma$-rays decreases to $\tau_{\gamma\gamma} \lesssim 1$ by the time of Cherenkov telescope observations (say, at $t \sim 10^2$ s into the afterglow phase) imposes a restriction on the energy budget of the GRB propagating through relatively dense medium (or, equivalently, on the density of the medium for a GRB with a fixed energy budget) [30]. Re-interpreting the condition $\tau_{\gamma\gamma} \le 1$ from Eq. (9) as a lower bound on $\Gamma_0 \ge \Gamma$,

$$\Gamma > 200 \left[\frac{L_\epsilon}{10^{51}\ \text{erg/s}}\right]^{1/6} \left[\frac{t}{7\ \text{s}}\right]^{-1/6}, \quad (10)$$

and using a measurement of $t_0$, one can use Eqs. (3), (4) to estimate a lower bound on the total energy of the outflow $\mathcal{E}_0$:

$$\mathcal{E}_0 = \frac{t_0^{3-\gamma}\Gamma_0^4 m_p n_0 \Omega R_*^2}{(3-\gamma)^{3-\gamma}} > 10^{54} \left[\frac{\Omega}{0.1}\right] \left[\frac{t_0}{7\ \text{s}}\right]^{1/3} \times \\ \times \left[\frac{n_0}{10^{13}\ \text{cm}^{-3}}\right] \left[\frac{R_*}{10^{12}\ \text{cm}}\right]^2 \times \\ \times \left[\frac{L_\epsilon}{10^{51}\ \text{erg/s}}\right]^{2/3} \text{erg}, \quad (11)$$

where we have assumed $t \sim t_0$ for the time moment when $\tau_{\gamma\gamma} \sim 1$ (in general the two times are not necessarily equal).

Using the estimate $D \approx 2.4$ Gpc for the luminosity distance to the GRB190114C at $z = 0.4245$ as a reference, we find an estimate of the flux of the VHE $\gamma$-ray signal from the decelerating phase

$$\mathcal{F}_{pp} = \frac{\mathcal{L}_{pp}}{\Omega D^2} \simeq 10^{-8} \left[\frac{\Omega}{0.1}\right]^{-1/2} \times \\ \times \left[\frac{t}{10^2\ \text{s}}\right]^{-3/2} \left[\frac{\mathcal{E}_0}{10^{54}\ \text{erg/s}}\right]^{1/2} \left[\frac{n_0}{10^{13}\ \text{cm}^{-3}}\right]^{3/2} \times \\ \times \left[\frac{R_*}{10^{12}\ \text{cm}}\right]^3 \left[\frac{D}{2.4\ \text{Gpc}}\right]^{-2} \frac{\text{erg}}{\text{cm}^2\cdot\text{s}}. \quad (12)$$

This level of $\gamma$-ray flux is not far from the observed flux of GRB190114C in the $10^2 < t < 10^3$ s time interval, as can be seen from Fig. 1 [32] for the reference parameters of the wind density and overall energy output in our reference model. The VHE $\gamma$-ray flux of GRB190114C has decreased as $t^{-1.5}$ during the afterglow phase. This is close to the expected luminosity from $pp$ interactions for a GRB outflow expanding into environment with radial density profile with $\gamma = 2$. Figure 2 shows a model of expected time evolution of the VHE $\gamma$-ray spectrum of pion decay flux based on AAfrag parameterisation of the differential production cross-sections of $pp$ interactions [27]. The model $\gamma$-ray lightcurve in fixed energy range 0.3–1 TeV extracted from the the numerical calculation with AAfrag for the reference model considered in the text is shown in Fig. 1. It shows deviation from the $t^{-3/2}$ powerlaw behavior.

Even though the pion decay emission is not the only possible contribution to the VHE band $\gamma$-ray luminosity, the VHE band detection can serve as a selection criterion of GRBs that might be expanding into dense circumstellar environment and thus can be considered as candidate neutrino sources. This can be used in the multi-messenger neutrino + $\gamma$-ray analysis: the sensitivity of the neutrino searches can be improved if only GRBs with VHE $\gamma$-ray afterglow detection are used in the stacking analysis of neutrino signal.

GRB 190114C provides a useful example of such an approach. The measured TeV band $\gamma$-ray flux provides an upper limit on the pion decay flux in $10^2$–$10^3$ s interval. This in turn provides an upper bound on the neutrino flux, because the two fluxes are comparable during the deceleration phase when the GRB is transparent to the VHE $\gamma$-rays. Extrapolating this bound on neutrino flux back in time, to the prompt emission phase during which the VHE $\gamma$-ray flux is not detectable, one can find that the VHE $\gamma$-ray flux estimate $\sim 10^{-8}$ erg/cm$^2\cdot$s some $\sim 100$ s after the burst (12) suggests an estimate of $\lesssim 0.1$ neutrino events in a 10 km$^3$ scale neutrino detector (9).

We have considered conditions for observability of $\gamma$-ray and neutrino emission from proton–proton interactions in the GRB outflow propagating through the circumstellar medium of the GRB progenitor star. We find that if the star has been suffering from significant mass loss rate, or was a part of a binary system, the *pp* interactions could generate detectable neutrino and $\gamma$-ray flux from the GRB afterglow. We have used the stellar evolution modelling of Ref. [21] to derive a possible range of single progenitor star parameters (initial mass and metallicity) in which the neutrino signal from *pp* interactions might be detectable with current and next-generation neutrino telescopes. Applying the estimates of the flux to the GRBs detected in VHE $\gamma$-rays by the ground-based $\gamma$-ray telescopes we have found that their $\gamma$-ray afterglows might have a sizeable contribution of *pp* interactions to their flux. Measurements of the VHE $\gamma$-ray flux of GRB 190114C impose upper limits on its neutrino fluence. We have shown that the fluence of neutrinos from *pp* interactions from the GRB propagation through the circumstellar medium in this source is too small to be detectable even with 10 km$^3$ scale neutrino detector like IceCube-Gen2.

**Funding.** This work is supported by the Ministry of science and higher education of Russian Federation under the contract 075-15-2020-778 in the framework of the Large scientific projects program within the national project “Science”.

*The full text of this paper is published in the English version of JETP.*

## REFERENCES

**1**. K. Davidson and R. M. Humphreys, Ann. Rev. Astron. Astrophys. **35**, 1 (1997), https://doi.org/10.1146/annurev.astro.35.1.1, URL https:// doi.org/10.1146/annurev.astro.35.1.1.

**2**. B. Paczyński, Astrophys. J. **494**, L45 (1998), URL https://doi.org/10.1086%2F311148.

**3**. T. Piran, Phys. Rep. **314**, 575 (1999); arXiv:astro-ph/9810256.

**4**. P. Kumar and B. Zhang, Phys. Rep. **561**, 1 (2015); arXiv:1410.0679.

**5**. P. Meszaros and M. J. Rees, Month. Not. Roy. Astron. Soc. **269**, L41 (1994); arXiv:astro-ph/ 9404056.

**6**. H. Abdalla, R. Adam, F. Aharonian, F. Ait Benkhali, E. O. Angüner, M. Arakawa, C. Arcaro, C. Armand, H. Ashkar, M. Backes et al., Nature **575**, 464 (2019), URL https://doi.org/10.1038/s41586-019-1743-9.

**7**. H. Abdalla, R. Adam, F. Aharonian, F. Ait Benkhali, E. O. Angüner, M. Arakawa, C. Arcaro, C. Armand, H. Ashkar, M. Backes et al., Nature (London) **575**, 464 (2019); arXiv:1911.08961.

**8**. V. A. Acciari, S. Ansoldi, L. A. Antonelli, A. Arbet Engels, D. Baack, A. Babić, B. Banerjee, U. Barres de Almeida, J. A. Barrio, J. Becerra González et al., Nature **575**, 455 (2019), URL https://doi.org/10.1038/s41586-019-1750-x.

**9**. V. A. Acciari, S. Ansoldi, L. A. Antonelli, A. A. Engels, D. Baack, A. Babić, B. Banerjee, U. Barres de Almeida, J. A. Barrio, J. B. González et al., Nature **575**, 459 (2019), URL https://doi.org/10.1038/s41586-019-1754-6.

**10**. R. Sari, T. Piran, and R. Narayan, Astrophys. J. Lett. **497**, L17 (1998); arXiv:astro-ph/9712005.

**11**. L. Nava, Int. J. Mod. Phys. D **27**, 1842003 (2018); arXiv:1804.01524.

**12**. X.-Y. Wang, R.-Y. Liu, and M. Lemoine, Astrophys. J. **771**, L33 (2013); arXiv:1305.1494.

**13**. Q.-W. Tang, P.-H. T. Tam, and X.-Y. Wang, Astrophys. J. **788**, 156 (2014); arXiv:1405.0451.

**14**. E. Waxman and J. Bahcall, Phys. Rev. Lett. **78**, 2292 (1997), URL https://link.aps.org/doi/10.1103/ PhysRevLett.78.2292.

**15**. J. I. Katz, Astrophys. J. Lett. **432**, L27 (1994); arXiv: astro-ph/9405033.

**16**. B. Paczynski and G. Xu, Astrophys. J. **427**, 708 (1994).

**17**. M. Ostrowski and A. A. Zdziarski, Astrophys. Space Sci. **231**, 339 (1995).

**18**. F. Halzen and G. Jaczko, Phys. Rev. D **54**, 2779 (1996).

**19**. A. Heger, S. E. Woosley, C. L. Fryer, and N. Langer, in *From Twilight to Highlight*: *The Physics of Supernovae*, Springer (2003), pp. 3–12, URL http://dx.doi.org/ 10.1007/10828549_1.

**20**. M. J. Barlow, L. J. Smith, and A. J. Willis, Month. Not. Roy. Astron. Soc. **196**, 101 (1981).

**21**. J. J. Eldridge, F. Genet, F. Daigne, and R. Mochkovitch, Month. Not. Roy. Astron. Soc. **367**, 186 (2006), https://academic.oup.com/mnras/article-pdf/367/1/186/6389625/367-1-186.pdf, URL https://doi.org/10.1111/j.1365-2966.2005.09938.x.

**22**. K. Belczynski, M. Dominik, T. Bulik, R. O'Shaughnessy, C. Fryer, and D. E. Holz, Astrophys. J. Lett. **715**, L138 (2010); arXiv:1004.0386.

**23**. P. A. Crowther, Ann. Rev. Astron. Astrophys. **45**, 177 (2007), https://doi.org/10.1146/annurev.astro.45.051806.110615, URL https://doi.org/10.1146/ annurev.astro.45.051806.110615.

**24**. L. Sironi, U. Keshet, and M. Lemoine, Space Sci. Rev. **191**, 519 (2015); arXiv:1506.02034.

**25**. R. D. Blandford and C. F. McKee, Phys. Fluids **19**, 1130 (1976).

**26**. S. R. Kelner, F. A. Aharonian, and V. V. Bugayov, Phys. Rev. D **74**, 034018 (2006); arXiv:astro-ph/0606058.

**27**. M. Kachelrieß, I. V. Moskalenko, and S. Ostapchenko, Comput. Phys. Comm. **245**, 106846 (2019); arXiv: 1904.05129.

**28**. S. R. Kelner, F. A. Aharonian, and V. V. Bugayov, Phys. Rev. D **74**, 034018 (2006); arXiv:astro-ph/0606058.

**29**. P. Bhattacharjee and N. Gupta, Astropart. Phys. **20**, 169 (2003); arXiv:astro-ph/0211165.

**30**. E. Derishev and T. Piran, Astrophys. J. **880**, L27 (2019), URL http://dx.doi.org/10.3847/2041-8213/ab2d8a.

**31**. M. Ajello, M. Arimoto, M. Axelsson, L. Baldini, G. Barbiellini, D. Bastieri, R. Bellazzini, A. Berretta, E. Bissaldi, R. D. Blandford et al., Astrophys. J. **890**, 9 (2020); arXiv:1909.10605.

**32**. MAGIC Collaboration, V. A. Acciari, S. Ansoldi, L. A. Antonelli, A. A. Engels, D. Baack, A. Babić, B. Banerjee, U. Barres de Almeida, J. A. Barrio et al., Nature (London) **575**, 459 (2019); arXiv:2006.07251.